Supporting Information

Towards Efficient and Stable Perovskite Solar Cells Employing Non-Hygroscopic F4-TCNQ doped TFB as Hole-Transporting Material

Hannah Kwon,‡[a] *Ju Won Lim,*‡[a,b] *Jinyoung Han,*[a] *Li Na Quan,*[c] *Dawoon Kim,*[d] *Eun-Sol Shin,*[e] *Eunah Kim,*[f] *Dong-Wook Kim,*[f] *Yong-Young Noh,*[e] *In Chung*[d] *and Dong Ha Kim**[a,g]

[a]Department of Chemistry and Nano Science, Ewha Womans University, 52, Ewhayeodae-gil, Seodaemun-gu, Seoul 03760, Republic of Korea

[b]Department of Materials Science and Engineering, University of Michigan, Ann Arbor, 48109, USA

[c]Department of Chemistry, University of California, Berkeley, California 94720, United States

[d]School of Chemical and Biological Engineering, Seoul National University, Seoul 08826, Republic of Korea

[e]Department of Chemical Engineering, Pohang University of Science and Technology (POSTECH), Pohang, Gyeongbuk, 37673, Republic of Korea

[f]Department of Physics, Ewha Womans University, 52, Ewhayeodae-gil, Seodaemun-gu, Seoul 03760, Republic of Korea

[g]Division of Chemical Engineering and Materials Science, Ewha Womans University, 52 Ewhayeodae-gil, Seodaemun-gu, Seoul 03760, Republic of Korea.

‡ This authors contributed equally.

*To whom correspondence should be addressed.

Tel.: +82-2-3277-4517; Fax: +82-2-3277-4546

E-mail: dhkim@ewha.ac.kr

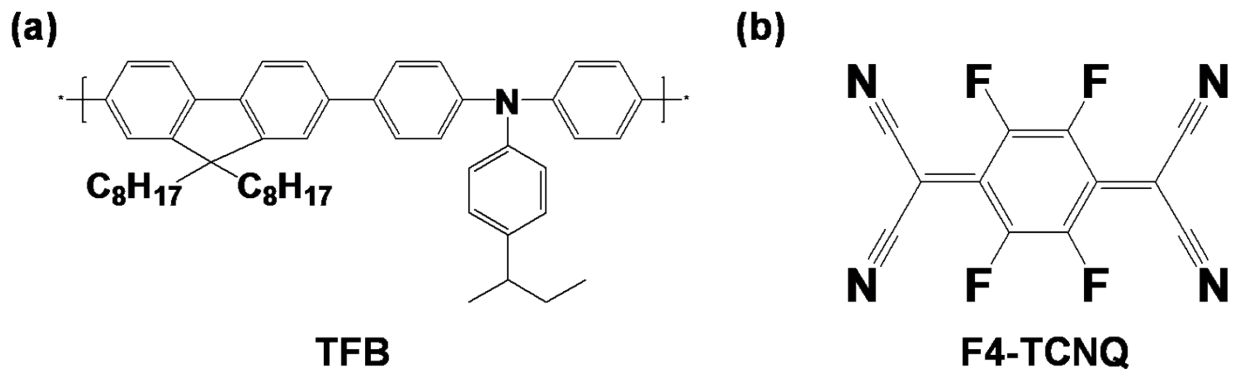

Figure S1. Chemical structure of (a) TFB and (b) dopant F4-TCNQ.

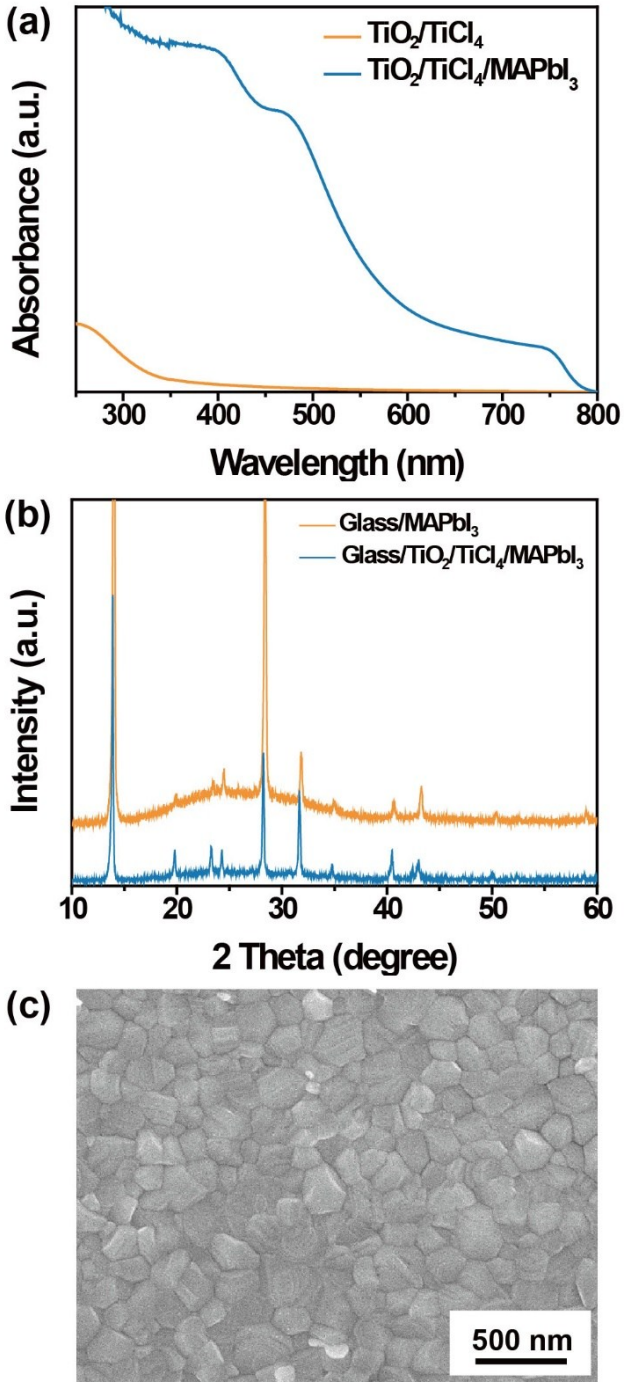

Figure S2. (a) UV-vis absorbance spectra of $TiO_2/TiCl_4$ layer and $TiO_2/TiCl_4$/Perovskite layer. (b) XRD spectrum of the perovskite and $TiO_2/TiCl_4$/Perovskite surface coated on the glass substrate. (c) SEM image of perovskite surface.

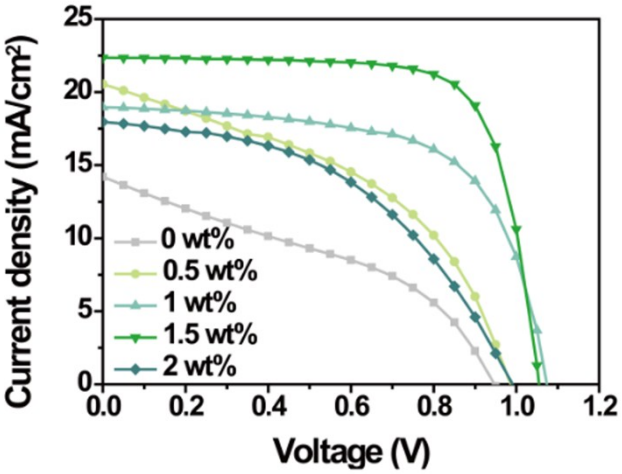

Figure S3. Photovoltaic performance of PCSs based on TFB with increasing F4-TCNQ dopant concentration under AM 1.5 G illumination.

Table S1. Average value of the photovoltaic performance parameters for 10 devices based on different dopant concentrations of F4-TCNQ. The parentheses in the table denote the maximum efficiency among the devices.

Doping Ratio (mol%)	**Voc (V)**	**J_{SC} (mA/cm^2)**	**Fill Factor**	**Efficiency (%)**
0%	0.84 ± 0.08 (0.94)	12.57 ± 2.96 (21.84)	33.60 ± 4.23 (38.67)	3.59 ± 1.10 (5.20)
0.5%	0.97 ± 0.02 (0.98)	18.73 ± 3.21 (20.55)	45.25 ± 6.01 (44.08)	8.06 ± 0.57 (8.94)
1%	1.02 ± 0.04 (1.07)	18.11 ± 0.78 (18.97)	61.67 ± 3.92 (63.48)	11.41 ± 0.74 (12.93)
1.5%	1.06 ± 0.02 (1.05)	22.22 ± 0.42 (22.36)	71.81 ± 1.37 (74.03)	16.86 ± 0.32 (17.46)
2%	0.93 ± 0.07 (0.94)	16.54 ± 2.15 (17.82)	47.24 ± 6.38 (50.78)	7.19 ± 0.75 (8.51)

Table S2. Statistical data of photovoltaic performance of PCSs based on TFB with different dopant concentrations of F4-TCNQ under AM 1.5 G illumination (a) 0%, (b) 0.5%, (c) 1%, (d) 1.5%, and (e) 2%, respectively. The best performance of the device is emphasized in red.

(a)

Voc (V)	Jsc (mA/cm^2)	Fill Factor	Efficiency (%)
0.94	14.19	38.67	5.20
0.82	14.68	35.44	4.27
0.78	14.05	34.00	3.75
0.77	15.48	36.21	4.36
0.82	7.92	29.67	1.94
0.71	8.07	36.35	2.11
0.92	11.45	30.84	3.26
0.91	12.64	36.71	4.26
0.93	10.78	24.45	2.47
0.77	16.42	33.70	4.30

(b)

Voc (V)	Jsc (mA/cm^2)	Fill Factor	Efficiency (%)
0.98	20.55	44.08	8.94
0.91	23.65	36.76	7.88
0.96	14.02	53.93	7.30
0.99	17.92	47.67	8.54
0.95	20.93	37.53	7.51
0.97	20.39	43.28	8.57
0.97	22.06	39.58	8.56
0.95	16.36	47.27	7.39
0.99	15.49	51.40	7.89
0.98	15.96	51.01	7.97

(c)

Voc (V)	Jsc (mA/cm^2)	Fill Factor	Efficiency (%)
1.07	18.97	63.48	12.93
1.06	19.12	54.25	10.97
1.04	17.44	62.85	11.40
1.08	19.01	59.01	12.10
1.02	17.18	66.64	11.66
0.97	17.48	65.62	11.18
0.96	18.79	58.31	10.54
1.03	17.28	60.18	10.76
1.01	17.97	65.74	11.87
0.99	17.84	60.60	10.71

(d)

Voc (V)	Jsc (mA/cm^2)	Fill Factor	Efficiency (%)
1.05	22.36	74.03	17.46
1.07	22.00	71.55	16.84
1.00	22.54	73.61	16.57
1.08	22.81	69.23	17.13
1.05	22.65	71.44	17.05
1.08	22.31	70.96	17.17
1.05	22.35	70.94	16.70
1.04	22.07	72.38	16.64
1.07	21.63	71.84	16.56
1.06	21.50	72.11	16.49

(e)

Voc (V)	Jsc (mA/cm^2)	Fill Factor	Efficiency (%)
0.99	17.96	46.79	8.33
0.88	18.96	40.44	6.78
0.75	14.95	59.04	6.69
0.97	17.95	38.51	6.72
0.93	17.73	47.61	7.92
0.91	17.79	50.97	8.28
0.96	16.70	45.26	7.28
0.98	11.57	54.84	6.27
0.99	15.33	41.83	6.41
0.93	16.43	47.13	7.22

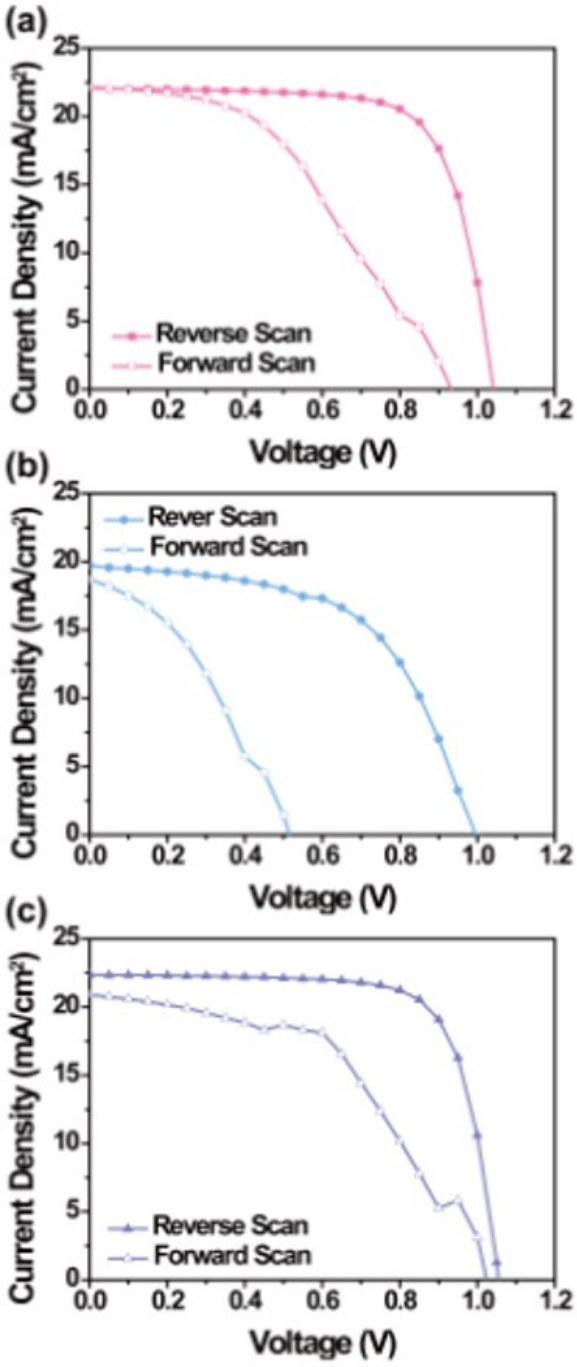

Figure S4. Hysteresis of the (a) $MAPbI_3$/Spiro-OMeTAD (LiTFSI + TBP), (b) $MAPbI_3$/TFB (LiTFSI + TBP), (c) $MAPbI_3$/TFB (F4-TCNQ) films.

Table S3. Hysteresis of the photovoltaic performance parameters.

Type of HTLs	Voc (V)	Jsc (mA/cm^2)	Fill Factor	Efficiency (%)	Hysteresis Index
Spiro-OMeTAD (LiTFSI + TBP)	1.02 ± 0.02 (1.04)	22.18 ± 0.41 (22.07)	68.74 ± 1.44 (72.38)	15.62 ± 0.45 (16.64)	0.295
TFB (LiTFSI + TBP)	0.96 ± 0.05 (0.99)	18.72 ± 1.09 (19.72)	51.91 ± 3.64 (56.04)	9.40 ± 0.90 (11.01)	0.588
TFB (F4-TCNQ)	1.06 ± 0.02 (1.05)	22.05 ± 0.47 (22.36)	71.05 ± 1.61 (74.03)	16.58 ± 0.41 (17.46)	0.257

$$\text{Hysteresis Index (HI)} = \frac{\int_{SC}^{OC} (J_{RS}(V) - J_{FS}(V))dV}{\int_{SC}^{OC} J_{RS}(V)dV}$$

$\int_{SC}^{OC} J_{FE}(V)dV$ and $\int_{SC}^{OC} J_{RS}(V)dV$ represents the integrated area under J−V curves under forward and reverse scans.

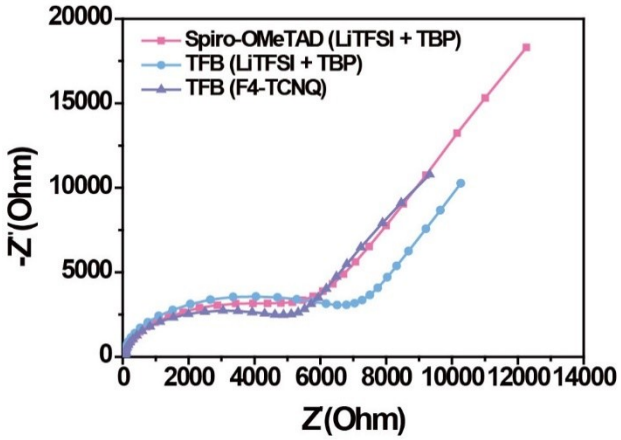

Figure S5. Nyquist plots of the PSC devices with different HTLs in whole region.

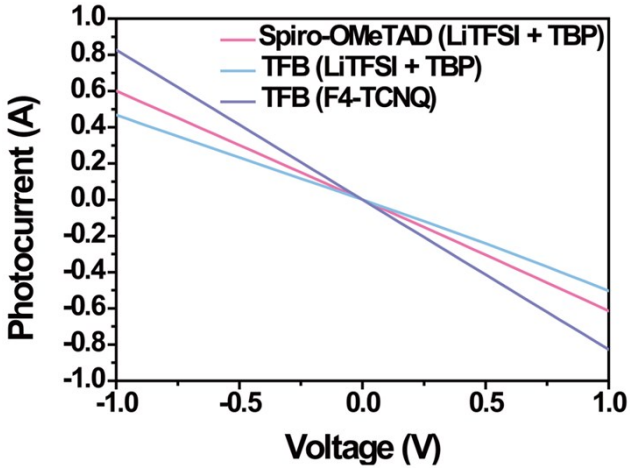

Figure S6. I-V curves of the three different hole transport layer only devices.

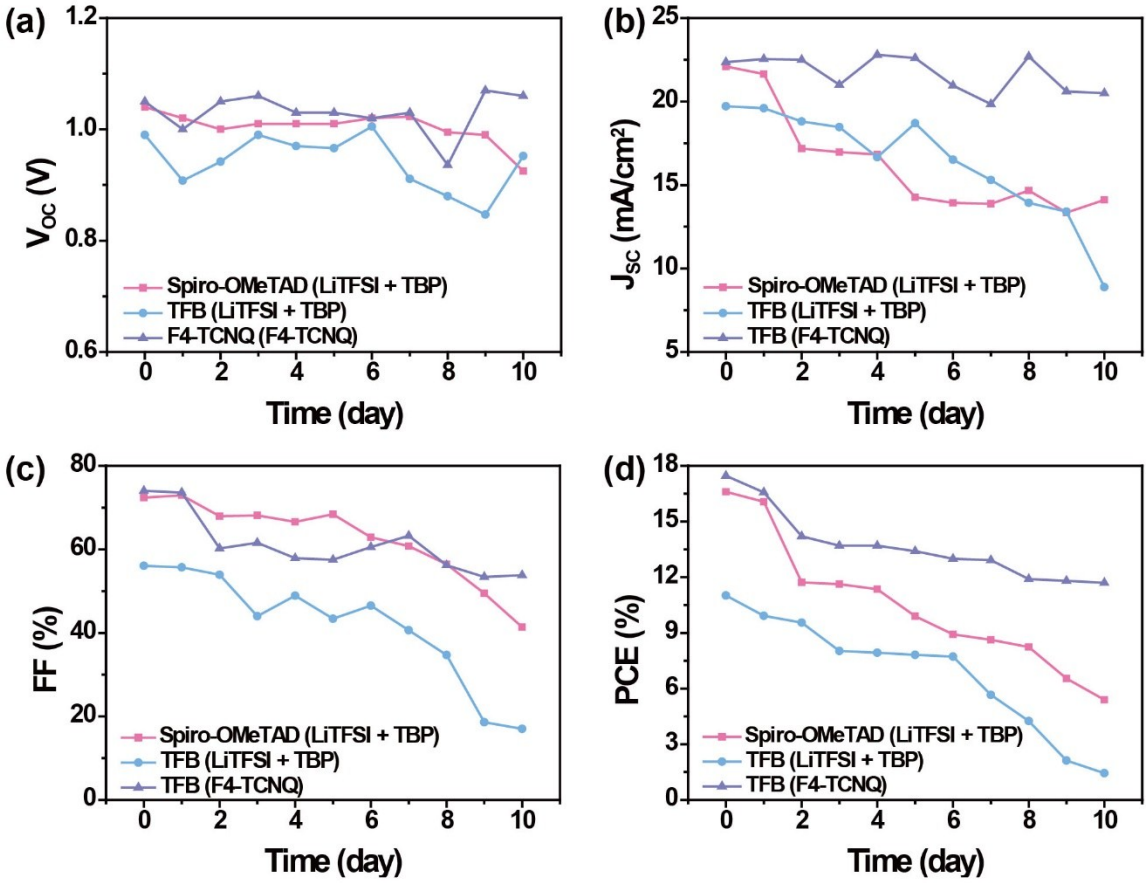

Figure S7. Photovoltaic decay curve for the perovskite solar cells in air atmosphere with humidity of about 45%.

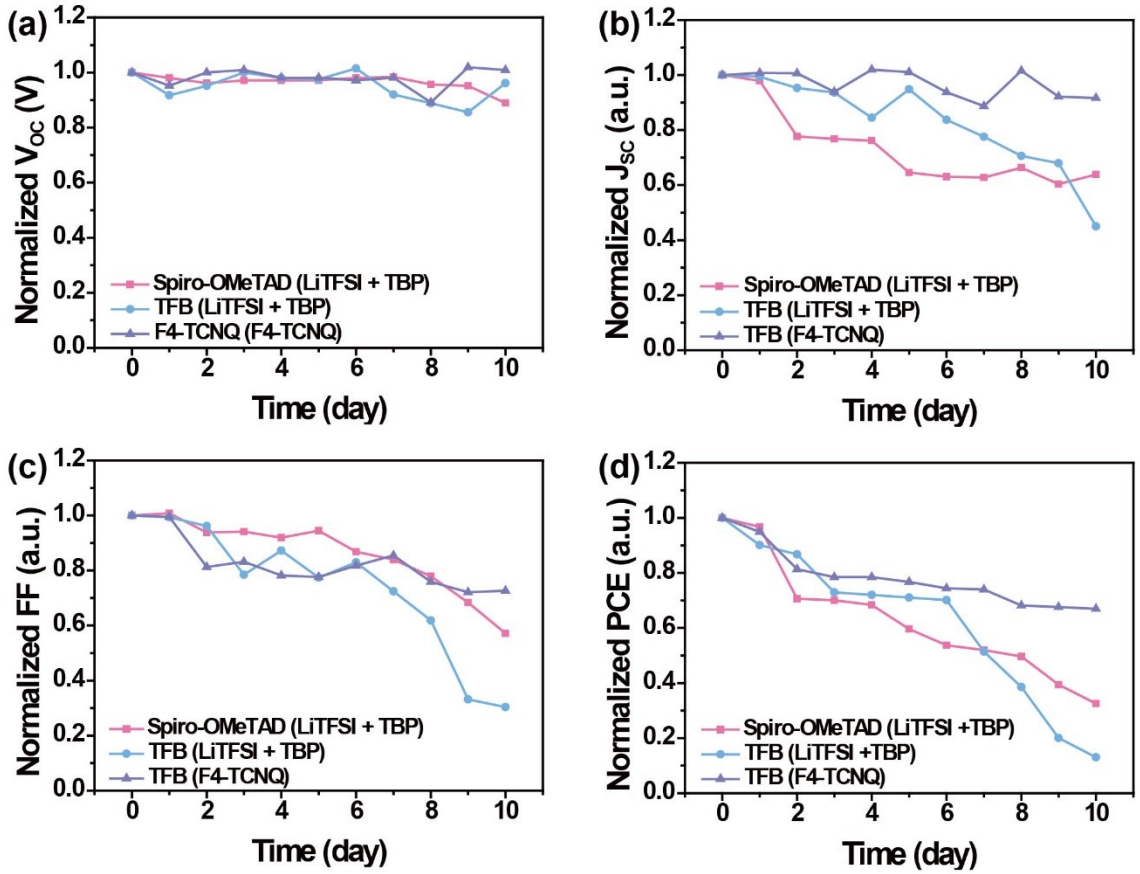

Figure S8. Normalized photovoltaic decay curve for the perovskite solar cells in air atmosphere with humidity of about 45%.

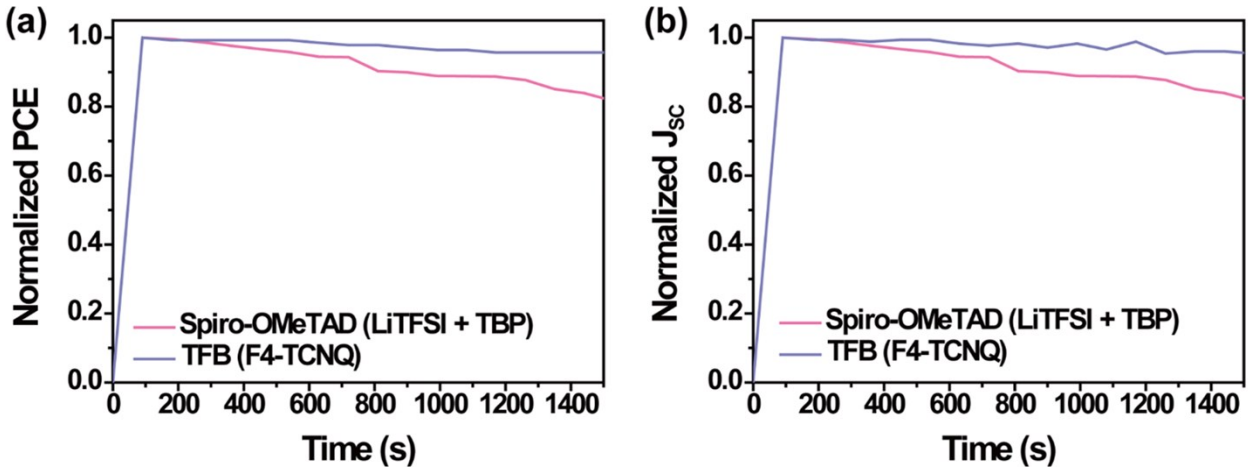

Figure S9. The steady state power output of a representative PSC devices based on Spiro-OMeTAD (LiTFSI + TBP) and TFB (F4-TCNQ) was measured at a constant bias of 0.75 and 0.8 V, respectively.

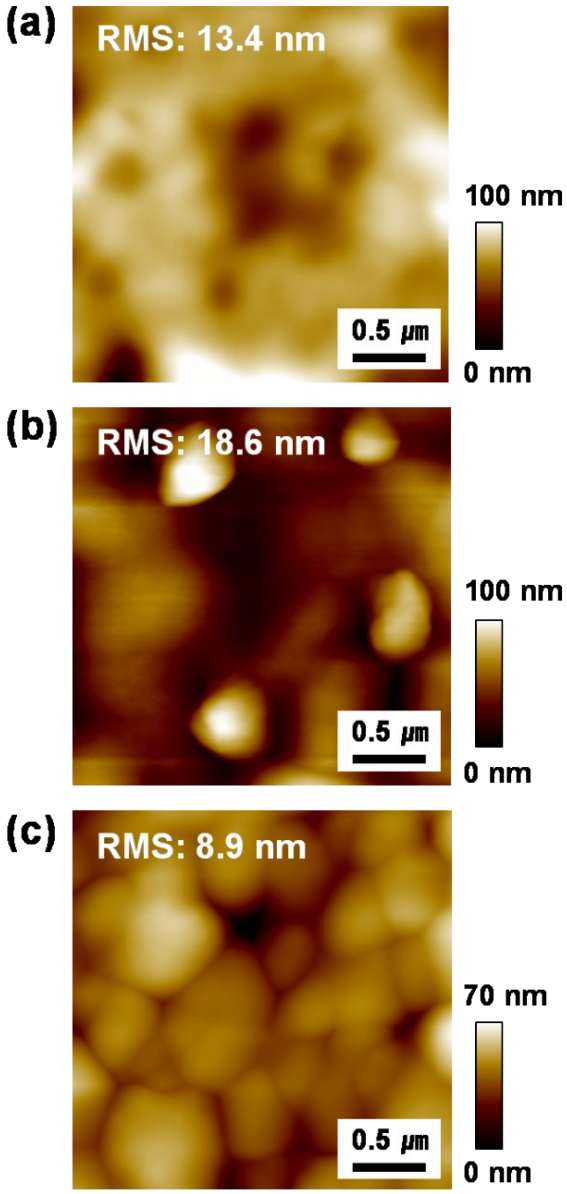

Figure S10. AFM images of the (a) $MAPbI_3$/Spiro-OMeTAD (LiTFSI + TBP), (b) $MAPbI_3$/TFB (LiTFSI + TBP), (c) $MAPbI_3$/TFB (F4-TCNQ) films.

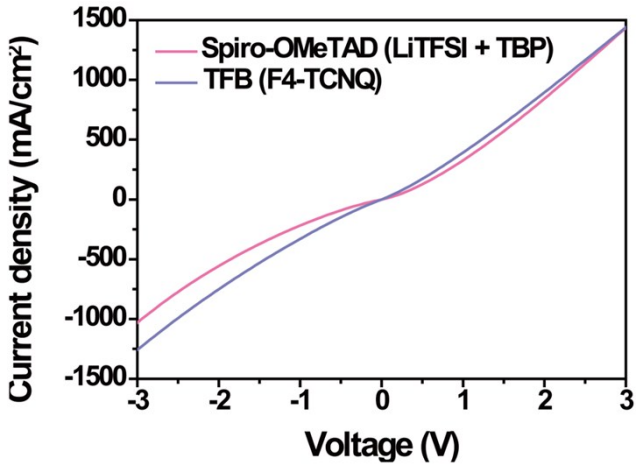

Figure S11. Current density versus applied voltage measured by holy-only devices at room temperature.

To calculate the hole mobility, Mott's Space charge-limited current (SCLC) method was carried out. The measured current follows Mott–Gurney's square law

$$J_D = \frac{9\varepsilon_0\epsilon_r\mu V^2}{8L^3}$$

where V is applied voltage, J is dark current, L is the thickness of the HTM layer, ε_0 is the vacuum permittivity and ε_r is relative dielectric constants, respectively.

Table S4. Statistical data of photovoltaic parameters for 20 PSC devices. The device configuration is FTO/TiO_2/$TiCl_4$/Perovskite/Spiro (LiTFSI + TBP)/Au. The best performance of the device is highlighted in red.

Voc (V)	Jsc (mA/cm^2)	Fill Factor	Efficiency (%)
1.02	22.25	64.67	14.67
1.02	21.64	72.95	16.06
1.02	22.09	70.67	15.87
0.99	22.40	64.55	14.28
1.00	21.84	71.77	15.61
1.04	22.07	72.38	16.64
1.04	22.82	68.10	16.15
1.03	22.64	68.55	16.06
1.04	22.61	68.65	16.19
1.05	22.63	67.38	16.07
1.00	21.38	70.43	15.01
1.01	22.33	66.58	15.03
1.00	22.17	69.79	15.53
1.03	22.20	67.16	15.42
1.04	21.78	68.37	15.49
1.05	21.71	67.04	15.37
1.03	21.59	68.84	15.32
1.02	22.83	68.46	15.91
1.01	22.45	69.22	15.63
1.04	22.24	69.30	16.00

Table S5. Statistical data of photovoltaic parameters for 20 PSC devices. The device configuration is FTO/TiO_2/$TiCl_4$/Perovskite/TFB (LiTFSI + TBP)/Au. The best performance of the device is highlighted in red.

Voc (V)	Jsc (mA/cm^2)	Fill Factor	Efficiency (%)
0.95	20.38	50.76	9.87
0.88	17.39	49.92	7.66
0.99	18.19	57.80	10.43
0.95	19.93	54.93	10.47
0.92	19.76	48.37	8.85
1.03	18.01	48.65	9.03
0.99	19.72	56.04	11.01
0.96	19.58	50.41	9.52
0.89	18.11	52.20	8.41
0.93	18.83	46.41	8.17
1.01	18.58	51.79	9.77
1.03	18.71	56.11	10.81
0.88	20.11	53.07	9.43
0.94	18.08	52.81	9.40
0.93	19.77	48.37	8.85
0.97	19.58	50.42	9.52
1.03	18.01	48.65	9.03
0.99	17.20	47.82	8.15
0.99	18.02	53.73	9.62
1.01	16.43	59.92	9.96

Table S6. Statistical data of photovoltaic parameters for 20 PSC devices. The device configuration is FTO/TiO_2/$TiCl_4$/Perovskite/TFB (F4-TCNQ)/Au. The best performance of the device is highlighted in red.

Voc (V)	Jsc (mA/cm^2)	Fill Factor	Efficiency (%)
1.05	22.36	74.03	17.46
1.04	22.53	67.55	15.77
1.00	22.54	73.61	16.57
1.08	22.81	69.23	17.13
1.05	22.65	71.44	17.05
1.08	22.31	70.96	17.17
1.05	22.35	70.94	16.70
1.04	22.07	72.38	16.64
1.07	21.63	71.84	16.56
1.08	22.12	68.07	16.25
1.07	21.80	69.91	16.35
1.04	22.66	70.82	16.76
1.07	21.52	71.00	16.36
1.08	21.25	72.20	16.52
1.06	21.91	71.46	16.56
1.07	22.00	71.55	16.84
1.07	21.80	69.64	16.22
1.05	22.00	70.68	16.29
1.06	21.50	72.11	16.49
1.05	21.25	71.52	16.00

Table S7. Summary of the parameters from fitting to the TRPL measurement data.

	HTLs	A_1	τ_1 (ns)	A_2	τ_2 (ns)
(a)	Spiro-OMeTAD (LiTFSI + TBP)	1953.99	15.21	25.26	285.43
(b)	TFB (LiTFSI + TBP)	2661.66	45.86	1868.92	194.93
(c)	TFB (F4-TCNQ)	4773.01	3.75	250.13	43.08